


The anterior-posterior gradient of the fusiform gyrus modulates the transition between mnemonic and perceptual features during reminiscences

Received: 30 September 2024

Accepted: 22 July 2025

Published online: 13 August 2025

 Check for updates

Motong Yuan^{1,2,10}, Yanyan Li^{1,3,10}, Jing Wang⁴, Yufei Cai^{1,3}, Wenya Yang⁵, Mengyang Wang⁴, Bo Zhang^{6,7}, Hongwei Sun², Guoming Luan⁸, Georg Northoff⁹ & Liang Wang^{1,3} 

Our cognition can be oriented either towards the external environment, as in perception, or towards our own self and its memories. However, the perception-memory continuum underlying the construction of memories remains unclear. Addressing this gap in our knowledge is the goal of our study; for that we uniquely investigate a rare mental phenomenon, namely internally- and externally-oriented reminiscences as manifest in memories and experiential hallucinations. To probe the causality of precisely located areas in eliciting and structuring such perceptual-mnemonic interactions, we studied a large sample of 335 patients with electrodes implanted across nearly the entire cortical surface, combining intracranial electrical stimulation (iES) and electrophysiological causal connectivity. We demonstrate that the likelihood of internally-oriented reminiscences was significantly higher during stimulation of the anterior fusiform gyrus. Conversely, externally-oriented hallucinations were far more likely to occur upon stimulation of the posterior fusiform gyrus. The probability of connections from regions outside the fusiform gyrus that displayed internally-oriented reminiscences to the fusiform gyrus decreased along the anterior-posterior axis. This suggests that an anterior-posterior gradient within the fusiform gyrus mediates an analogous external-internal perceptual-mnemonic continuum.

The interplay between memory and perception is a central puzzle question in neuroscience^{1–5}, with disruptions in their push-pull dynamics implicated in hallucinations⁶ and recognition deficits^{7,8}. Recent work has demonstrated that the high-level visual cortex plays distinct yet coactive roles in both visual perception and recognition memory^{5,9,10}. For instance, retinotopy structures interactions between perceptual and mnemonic neural systems⁵. However, the perception-memory continuum underlying the construction of memories remains unclear.

A large body of neuroimaging studies has demonstrated that the fusiform gyrus, a key structure in high-level visual processing, is involved in different aspects of perception and memory^{11–14}. This may be due to the fact that the fusiform gyrus comprises distinct sub-regions that serve complementary roles^{15,16}. For instance, intracranial electrical stimulation (iES) to posterior and middle sections along the anterior-posterior axis of the fusiform gyrus has been shown to induce perceptual distortion^{17,18} or elicit visual sensation^{18,19}. While observations in two single case reports showed that stimulation to the anterior

fusiform gyrus may lead to a transient memory impairment but not perceptual changes^{20,21}. Thus, the anterior-posterior axis of the fusiform gyrus might play a pivotal role in the perceptual-mnemonic interaction underlying the construction of memories in our reminiscences.

Notably, iES of mesial and lateral temporal structures in awake neurosurgical patients can elicit vivid reminiscences, ranging from internally-oriented familiarity/recollection to externally-oriented experiential hallucinations^{22–28}. This phenomenon provides a unique opportunity to probe the causal organization of perceptual-mnemonic processes along the fusiform gyrus. Here, we analyzed subjective experiences induced by iES in 335 patients with near-complete cortical coverage. Our study aimed to: (1) localize iES sites that elicit reminiscences, (2) identify distinct neuronal populations along the anterior-posterior fusiform axis associated with internally-oriented reminiscences versus externally-oriented hallucinations, and (3) determine whether efferents from other brain regions associated with internally-oriented reminiscences versus externally-oriented hallucinations synchronize distinct downstream connectivity patterns along the anterior-posterior axis of the fusiform gyrus, as the fusiform gyrus can be activated by external efferents²⁴. For the third objective, we utilized electrophysiological causal connectivity provided by the Functional Brain Tractography Project (F-Tract)^{29,30}.

Results

Three evaluators categorized the subjective reports of 335 patients (Supplementary Table 1) into different classifications based on the reported contents. The following are detailed definitions of different reminiscence categories.

Source dimension

Internally-oriented reminiscences: This category encompasses responses where patients perceived themselves as recalling past experiences or familiar individuals. The defining characteristic is the mental recreation of memories or familiarity, typically described as spontaneous thoughts or mental images. These experiences may not be associated with specific sensory perceptions but rather manifest as vivid or significant mental representations of past events.

Externally-oriented hallucinations: This category includes experiences perceived as external phenomena occurring within the visual field. Patients reported these experiences as though they were happening in the external environment, characterized by direct sensory perception that often resembled hallucinatory experiences.

Content dimension

Scenes: This category comprises memories or experiences primarily involving visual or sensory recollections of specific locations, environments, or situations, with particular emphasis on the overall setting.

People: This category includes experiences involving the recollection or perception of specific individuals, such as family members or acquaintances, with a focus on personal characteristics and identities.

Animals: This category consists of recollections or perceptions of animals, which may involve specific creatures, reported as distinct memories or hallucinations centered around animal-related experiences.

Objects: This category focuses on the recollection or experience of specific inanimate objects, typically items that are familiar to or have been encountered by the individual.

Scenes with People: This category includes experiences that combine both environmental settings and the presence of individuals within those settings, creating dynamic and contextually rich reminiscences.

Unclassified: This category was designated for experiences that could not be clearly categorized due to their fragmented, incomplete,

or ambiguous nature, often containing visual elements but lacking sufficient context for precise classification.

Quality dimension

Following the classification criteria established by Curot et al.²³ and contemporary memory theories³¹, we further categorized reminiscences as follows:

Semantic Memories: These represent general, culturally shared knowledge devoid of specific spatial or temporal context, constituting universally accessible information rather than personal historical experiences.

Personal Semantics: This category encompasses autobiographical knowledge without detailed recollection or temporal context, including recognized but not vividly recalled personal experiences that lack specific spatial or temporal markers characteristic of episodic memory.

Familiarity: This category includes experiences where patients recognize objects, sounds, or individuals but cannot recall specific contextual details, characterized by a general sense of recognition without access to detailed memory context.

Unclassified: This category contains responses involving visual content potentially related to memory but lacking sufficient detail for precise classification, often due to limited debriefing opportunities or insufficient information for evaluator consensus.

Notably, no stimulation resulted in mixed category responses. Please refer to Fig. 1a for direct quotes from patients describing their experiences. The process of classifying reported reminiscences is shown in Fig. 1b.

Stimulation induces reminiscences across the cortical surface. In total, reminiscences were elicited at 102 sites (0.3%) across 25 patients (7.5%), out of 30,404 stimulated sites tested in 335 patients (All reports of induced reminiscences and their classification, iES intensity, and MNI coordinates of all responsive sites are provided in Supplementary Table 2 and the raw data). The response rate here was consistent with a previous report²³. The spatial distribution of stimulated sites is illustrated in Fig. 2a, while the response sites categorized by source (Fig. 2b), content (Fig. 2c), and quality (Fig. 2d). Notably, since similar response rates were observed in the bilateral hemisphere ($\chi^2 = 0.090$, $p = 0.764$, Chi-squared Test), all electrode locations were projected to the left hemisphere to enhance visual recognition of the spatial patterns.

The responsive sites were predominantly concentrated in the medial temporal structures, lateral temporal lobe and insula (Fig. 3a). When high-frequency stimulation was applied to different sites, the stimulation current intensity required to elicit response varied (Fig. 3b), but the effective average current distribution exhibited no strong regional specificity (Fig. 3c). Electrical stimulation to multiple regions over the temporal lobe, insula, cingulate gyrus and putamen elicited responses in at least 2 patients (Fig. 3d). Most responses were observed in known visual memory-related regions (68/102, 66.7%), including the fusiform gyrus, medial and lateral temporal lobes (Fig. 3e). Significantly higher response rates were found in the fusiform gyrus compared to the reference structure (the superior temporal sulcus, which exhibited the lowest response rate), as determined by a linear mixed-effects (LME) model (LME, $t = 6.368$, $\beta = 0.017$, $SE = 0.003$, $p < 0.001$, Bonferroni correction, Table 1). Consequently, we further investigated the spatial characteristics of reminiscences in this region.

To demonstrate the specificity of the reminiscences induced by high-frequency stimulation, we also applied low-frequency stimulation to some of the patients receiving high-frequency stimulation. Among the 30,404 sites stimulated at 50 Hz across 335 patients, a total of 4971 sites (16.3%) from 140 patients (41.8%) also underwent 1 Hz stimulation (Fig. 3f and Supplementary Table 3). However, none of these

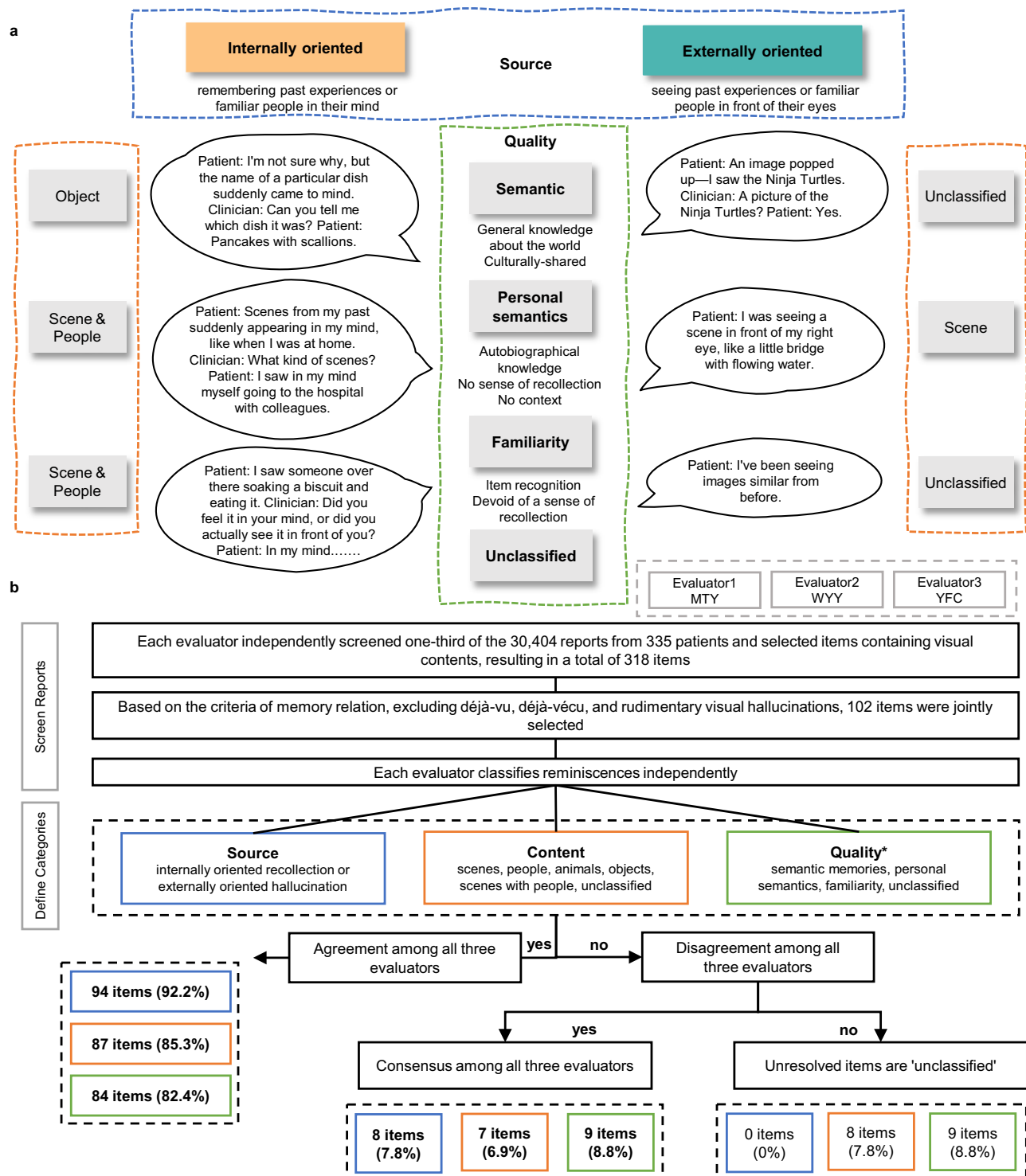


Fig. 1 | Examples and flowchart illustrating the process of classifying reported reminiscences. **a** Data categorization of memories induced by iES. Examples are provided for each category. **b** Three evaluators independently screened the subjective reports and selected the reports related to the visual contents. Then they consistently selected 102 memory-related items. The reminiscences were further

independently classified by the evaluators, and the final category corresponds to the consensus among the evaluators. *: Following the classification criteria outlined by Curot et al.²³, we categorized items into four of the eight categories. No items were classified as autobiographical episodic memories, personal folklore, reminiscence of a dream, or strangeness with memory.

1 Hz stimulations induced any reminiscence-like experiences. Furthermore, in five patients, seven sites that elicited reminiscences under 50 Hz stimulation yielded negative results when stimulated at 1 Hz.

Stimulation induces reminiscences across the fusiform gyrus. Among 1496 stimulated sites in 195 patients, the fusiform gyrus

showed 30 responsive sites (1.1%) across 17 patients (8.7%). These stimulated and responsive sites were distributed throughout the whole fusiform gyrus (Fig. 4a, b). Notably, despite a slight overlap between the rhinal cortex and fusiform gyrus, no responsive sites were located in both regions. The distribution of sites within the fusiform gyrus was further visualized in two-dimensions (anterior-posterior and medial-

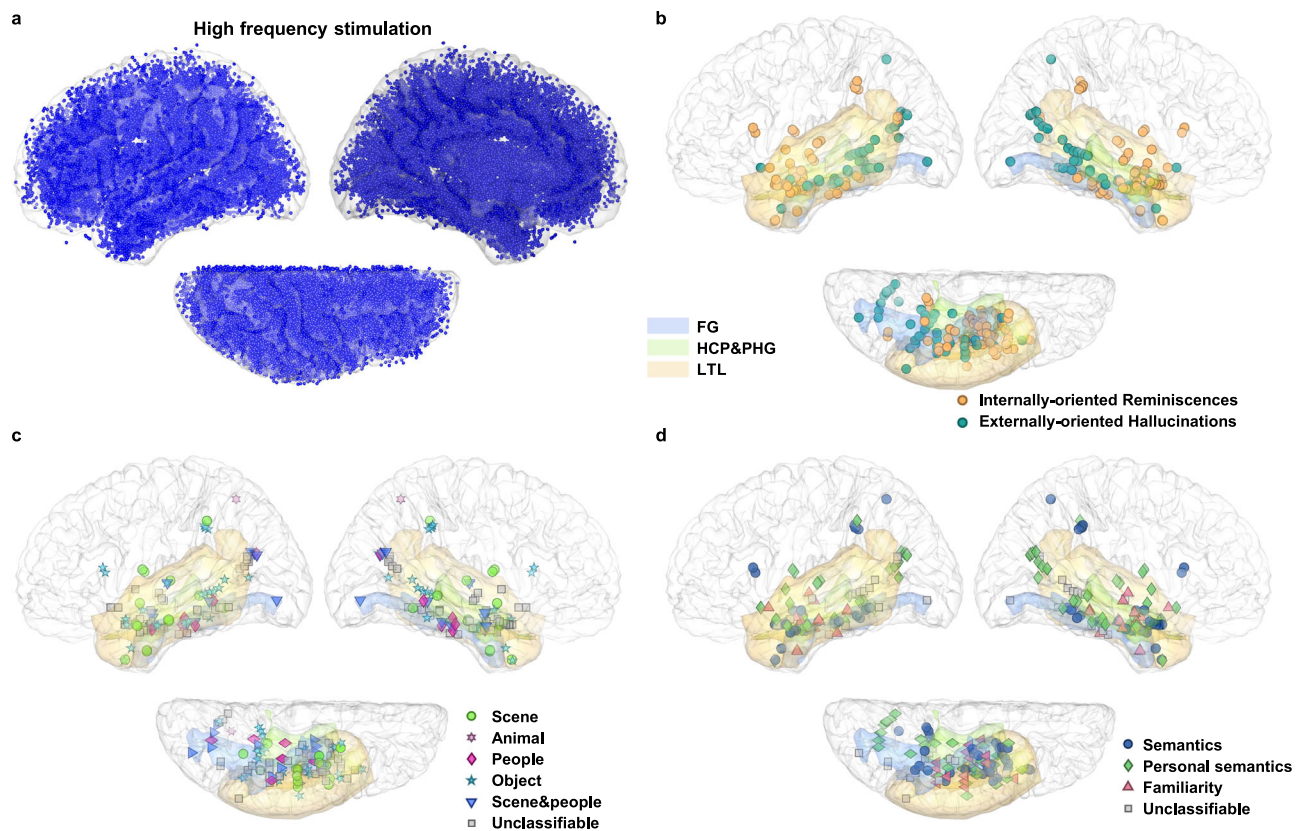


Fig. 2 | Distribution of stimulus sites across dimensions in the brain.

a Distribution of 50 Hz frequency stimulated sites ($n = 30,404$) from 335 patients. **b** Distribution of responsive sites categorized by source dimension: internally-oriented reminiscences (yellow circles) and externally-oriented hallucinations (cyan circles). **c** Distribution of responsive sites categorized by content dimension:

scene, animal, people, object, Scene & people, and unclassifiable. **d** Distribution of responsive sites categorized by quality dimension: semantics, personal semantics, familiarity and Unclassifiable. FG fusiform gyrus, HCP&PHG Hippocampus&Parahippocampal gyrus, LTL lateral temporal lobe.

lateral axes, Fig. 4c). Quantitative analysis using Receiver Operating Characteristic (ROC) curves revealed no significant variation in response probability along the anterior-posterior axis of the fusiform gyrus ($p = 0.857$, $AUC = 0.507$, permutation test, Fig. 4d, e). In contrast, response rates were higher on the lateral side compared to the medial side along the medial-lateral axis ($p = 0.012$, $AUC = 0.636$, permutation test, Fig. 4f, g). However, this observation may be influenced by the lower sampling rate on the medial side, requiring further investigation to clarify this effect.

The anterior-posterior axis of fusiform gyrus for perceptual-mnemonic transition underlying the reconstruction of memories.

Next, we investigated whether distinct neuronal populations along the anterior-posterior axis of the fusiform gyrus are associated with internally-oriented reminiscences versus externally-oriented hallucinations. Within the fusiform gyrus, 18 cases were internally-oriented reminiscences (60%), and 12 cases were externally-oriented hallucinations (40%). Figure 5a illustrates the spatial distribution of responsive sites associated with internally-oriented reminiscences and externally-oriented hallucinations. Notably, one patient reported both internally-oriented reminiscences and externally-oriented hallucinations along the fusiform gyrus, and the individual result was consistent with the group-level finding (Fig. 5b). For each memory type, a two-dimensional projection was generated along the medial-lateral and anterior-posterior axes, revealing distinct distribution patterns between the two memory types (Fig. 5c). Notably, we observed a transition from internally-oriented reminiscences to externally-oriented hallucinations along the anterior-posterior axis of the fusiform gyrus, but not along the medial-lateral axis. To further quantify this phenomenon, we

calculated the percentage of responses for each memory type and analyzed the oriented selectivity index (defined as the differential occurrences between internally-oriented reminiscences and externally-oriented hallucinations) along the medial-lateral and anterior-posterior axes of the fusiform gyrus. Consistent with our observations, internally-oriented reminiscences were predominantly localized in the anterior fusiform gyrus, whereas externally-oriented hallucinations were more frequently observed in the middle-posterior fusiform gyrus (Fig. 5d). These findings were robust and remained consistent across different binning configurations (Fig. S1). To validate the topographical organization of memory responses, we performed ROC analysis, which demonstrated that the anterior-posterior axis of the fusiform gyrus reliably predicted whether an internally-oriented reminiscence or an externally-oriented hallucination would be elicited ($p = 0.001$, $AUC = 0.819$, permutation test, Fig. 5e). In contrast, no significant trends were observed along the medial-lateral axis in the distribution of internally-oriented reminiscences versus externally-oriented hallucinations (Fig. 5f). This lack of differentiation was further confirmed by ROC analysis, which showed no significant difference along the medial-lateral axis ($p = 0.142$, $AUC = 0.625$, permutation test, Fig. 5g).

Furthermore, the anterior-posterior transition in the fusiform gyrus between mnemonic and perceptual features during reminiscences was not driven by memory content clustering, as different content categories were involved in both internally-oriented reminiscences and externally-oriented hallucinations (Fig. S2a, b). We calculated Euclidean distances within and between groups for different memory contents in the two types of memories. This analysis quantified spatial or feature-based dissimilarity, with smaller distances

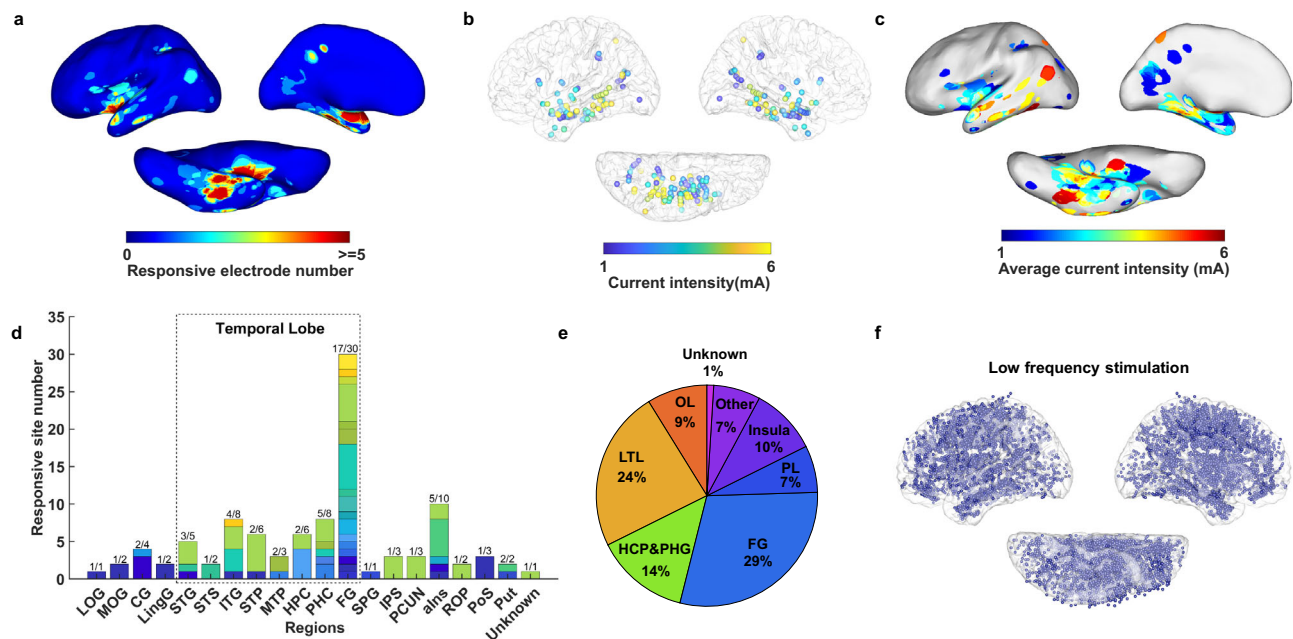


Fig. 3 | Induced reminiscence probability across the cortical surface. **a** Cortical surface mapping of responsiveness, with color gradients representing the density of responsive sites across brain regions. **b** Stimulation intensity parameters of responsive sites. **c** Cortical surface visualization of average current intensity, with data-deficient regions marked in grayish-white. **d** Responsiveness across cortical regions including at least one site that showed reminiscence to electrical stimulation (the ratio above each bar denotes #patient/#sites). **e** Proportion of responsive sites across the brain. **f** Distribution of 4971 low frequency stimulated sites from 140

patients. alns Anterior Insula, CG Calcarine Gyrus, FG Fusiform Gyrus, HPC Hippocampus, IPS Intraparietal Sulcus, ITG Inferior Temporal Gyrus, LingG Lingual Gyrus, LOC Lateral Occipital Cortex, LTL Lateral Temporal lobe, MOG Middle Occipital Gyrus, MTP Middle Temporal Pole, OL Occipital lobe, PCUN Precuneus, PHG Parahippocampal gyrus, PL Parietal lobe, PoS Parietooccipital Sulcus, Put Putamen, ROP Rolandic Operculum, SPC Superior Parietal Cortex, STG Superior Temporal Gyrus, STP Superior Temporal Pole, STS Superior Temporal Sulcus, Other = Regions not classified into the above brain areas.

indicating greater similarity (Fig. S2c). Statistical tests revealed no significant differences in distances between same-content and different-content conditions for either internally-oriented reminiscences or externally-oriented hallucinations (Mann-Whitney U test: all $p > 0.2$, Fig. S2d). Moreover, Euclidean distances for same-content and different-content conditions did not systematically vary across the oriented selectivity indices of the anterior, middle and posterior fusiform gyrus (Fig. S2e). These results suggest that the anterior-posterior gradient of the fusiform gyrus reflects a perceptual-mnemonic continuum independent of memory content. Additionally, the qualitative nature of memory did not influence our findings (Fig. S2f–j).

Notably, the current intensity required to elicit internally-oriented reminiscences was significantly lower than that for externally-oriented hallucinations (Mann-Whitney U test: $p < 0.01$, Fig. S3a). At 7 stimulated sites across three patients, the same memory content was consistently reported despite increases in electrical current intensity. In one additional patient, although the specific content varied with current intensity, the experience remained classified as internally-oriented reminiscences (Refer to the ‘Dose effect’ tab in the raw data file for details). This indicates that increased current intensity did not drive a shift between these two types of experiences. Furthermore, the anterior-posterior axis of the fusiform gyrus significantly influenced the occurrence of internally-oriented reminiscences and externally-oriented hallucinations ($F = 7.452$, $p = 0.011$, ANOVA), even after controlling for the current intensity. When analyzing all positive responses, there was no significant difference in current intensity between anterior and middle-posterior stimulations (Mann-Whitney U test: $p = 0.057$, Fig. S3b). However, across all stimulations, the current intensity for the anterior fusiform gyrus was significantly higher than for the posterior region (Mann-Whitney U test: $p < 0.001$, Fig. S3c). This suggests that the lower current intensity in the anterior fusiform gyrus was not due to clinical procedure biases. Nevertheless, we cannot rule out the possibility that higher stimulation intensities in the anterior

fusiform gyrus might activate remote neocortical areas, potentially eliciting externally-oriented hallucinations. Regardless, the anterior-posterior gradient of the fusiform gyrus remains a robust predictor of the distinction between internally-oriented reminiscences and externally-oriented hallucinations, independent of the confounding influence of gender, age, stimulation current intensity, memory content, and quality ($p = 0.001$, AUC = 0.977, permutation test, Fig. S4a).

Electrophysiological causal connectivity from other regions to the anterior-posterior axis of fusiform gyrus. Finally, we aimed to investigate whether the causal connectivity patterns between responsive sites outside the fusiform gyrus and the fusiform gyrus itself impacted the types of memory. By utilizing F-TRACT, we assessed the difference in the probability of responsive sites outside the fusiform gyrus connecting to both the fusiform and non-fusiform regions. The probability of connection to the fusiform gyrus was found to be higher than that to non-fusiform regions (Fig. 6a). Statistical analysis revealed a significant difference in the distribution of connection probabilities between the fusiform and non-fusiform regions (KS test: $D = 0.214$, $p = 1.799 \times 10^{-13}$). Additionally, a significant difference in the median connection probability between these regions was observed (Wilcoxon signed-rank test: $p = 1.473 \times 10^{-6}$, Fig. 6b). Furthermore, the probability of stimulated positive regions connecting to the fusiform gyrus was higher than that of regions without positive responses (KS test: $D = 0.176$, $p = 1.459 \times 10^{-19}$, Fig. 6c), and this difference was significant (Mann-Whitney U test: $p = 2.086 \times 10^{-11}$, Fig. 6d). These robust findings suggest that the fusiform gyrus may indeed function as a central hub within the reminiscence network, potentially serving as a critical node for integrating and processing memory-related information. We further revealed that the probability of connections from regions outside the fusiform gyrus associated with internally-oriented reminiscences to the fusiform gyrus decreased along the anterior-posterior axis (Fig. 6e), consistent with our fusiform gyrus mapping results. A biased

Table 1 | Distribution of reminiscences produced by brain region stimulation analyzed using a linear mixed effects model

Brain Region	n/N	Estimate (β)	SE	t	p	Bonferroni_p
Superior Temporal Sulcus	2/1377					
Lateral Occipital Cortex	1/556	−0.001	0.004	−0.377	0.706	1.000
Middle Occipital Gyrus	2/553	0.003	0.004	0.683	0.495	1.000
Calcarine Gyrus	4/607	0.003	0.004	0.934	0.350	1.000
Lingual Gyrus	2/384	0.002	0.004	0.578	0.563	1.000
Superior Temporal Gyrus	5/1439	−0.001	0.003	−0.436	0.663	1.000
Inferior Temporal Gyrus	8/1040	0.006	0.003	2.090	0.037	0.660
Superior Temporal Pole	6/237	0.015	0.005	2.953	0.003	0.057
Middle Temporal Pole	3/749	0.005	0.003	1.418	0.156	1.000
Hippocampus	6/725	0.005	0.003	1.342	0.180	1.000
ParaHippocampus	8/1071	0.004	0.003	1.245	0.213	1.000
Fusiform Gyrus	30/1496	0.017	0.003	6.368	1.971 × 10^{−10}	3.548 × 10^{−9}
Superior Parietal Cortex	1/265	0.004	0.005	0.723	0.470	1.000
Intraparietal Sulcus	3/576	−0.001	0.004	−0.217	0.828	1.000
Precuneus	3/1521	−0.001	0.003	−0.462	0.644	1.000
Parietooccipital Sulcus	3/630	0.003	0.004	0.930	0.353	1.000
Rolandic Operculum	2/1068	−0.002	0.003	−0.705	0.481	1.000
Anterior Insula	10/1862	0.002	0.003	0.884	0.377	1.000
Putamen	2/648	0.001	0.004	0.413	0.679	1.000

n and N represent the induced reminiscence sites and number of electrical stimulations in each brain region respectively. Estimated coefficient for the fixed effect of region relative to reference region. Brain regions in bold are those for which stimulation evoked significantly more reminiscences than reference region ($p < 0.05$, two-sided test). Source data are provided as a Source Data file.

connectivity selectivity index was used to quantify changes in connections between regions outside the fusiform gyrus and the anterior-posterior fusiform gyrus (Mann-Whitney U test: $p = 0.005$, Fig. 6f). The oriented selectivity index for internally-oriented reminiscences progressively decreased from the anterior to posterior fusiform gyrus (Fig. 6g). ROC analysis quantitatively verified the causal connectivity pattern from responsive sites to the anterior-posterior axis of fusiform gyrus, demonstrating that the oriented selectivity index predicted whether internally-oriented reminiscences or externally-oriented hallucinations were elicited ($p = 0.001$, AUC = 0.749, permutation test, Fig. 6h). This predictive capability remained robust and independent of potential confounding factors, including gender, age, stimulation current intensity, memory content, and quality ($p = 0.001$, AUC = 0.889, permutation test, Fig. S4b). These results indicated that functional connectivity patterns associated with internally-oriented reminiscences were more likely to target the anterior fusiform gyrus, while those associated with externally-oriented hallucinations were more likely to target the middle-posterior fusiform gyrus. Finally, we confirmed that the group-level findings were consistent with individual-level data (Fig. 6i–l). This individual-level pattern mirrored the group-level results, further supporting the robustness of the anterior-posterior connectivity gradient.

Additionally, to contextualize the findings from the fusiform gyrus within the broader framework of whole-brain connectivity, we examined whole-brain connection patterns. We selected the top 30 brain regions with the strongest overall connectivity, showing their connections with memory-related brain regions, particularly the lateral temporal lobe ($\chi^2 = 7.942$, $p = 0.005$, Chi-squared Test), the hippocampus and parahippocampal gyrus ($\chi^2 = 12.343$, $p = 4.427 \times 10^{-4}$, Chi-squared Test), and fusiform gyrus ($\chi^2 = 5.605$, $p = 0.018$, Chi-squared Test) (Fig. 6m). We then compared the connectivity strength between regions associated with internally-oriented reminiscences ($n = 36$) and externally-oriented hallucinations ($n = 16$) across these 30 brain regions. After Bonferroni correction, sites inducing externally-oriented hallucinations showed significantly increased functional connectivity to the middle fusiform gyrus (Mann-Whitney U test: $p = 0.009$, Bonferroni correction), the posterior middle temporal gyrus (Mann-Whitney U test: $p = 0.027$, Bonferroni

correction) and the middle inferior temporal gyrus (Mann-Whitney U test: $p = 0.035$, Bonferroni correction) (Fig. 6n). These findings were robust across different threshold (Fig. S5). In contrast, sites inducing internally-oriented reminiscences showed a slight but non-significant increase in functional connectivity to the anterior middle temporal pole (Mann-Whitney U test: $p = 0.024$, uncorrected) and posterior part of the anterior insula (Mann-Whitney U test: $p = 0.038$, uncorrected).

We also explored the topographical pattern of reminiscences in regions outside the fusiform gyrus. The internally-oriented reminiscences were more prevalent in anterior regions, such as the superior temporal pole and precuneus, while externally-oriented hallucinations appeared more frequently in posterior regions, such as the middle occipital gyrus and parietooccipital sulcus (Fig. 7a, b). It should be noted that the present findings predominantly rely on group-level population data, as elicited reminiscences are rare phenomena. Among the three patients who reported both internally-oriented reminiscences and externally-oriented hallucinations, two exhibited results consistent with the group-level analysis (Fig. 7c and Fig. S6). Quantitative analysis revealed that the oriented selectivity index varied along the anterior-posterior but not the medial-lateral axis, with internally-oriented reminiscences more prevalent anteriorly and externally-oriented hallucinations more frequent posteriorly (Fig. 7d, e). ROC analysis demonstrated that the anterior-posterior location of sites robustly predicted whether internally-oriented reminiscences or externally-oriented hallucinations were elicited ($p = 0.001$, AUC = 0.838, permutation test, Fig. 7f), whereas the medial-lateral position did not exhibit predictive value ($p = 0.069$, AUC = 0.613, permutation test, Fig. 7g). This internal-external gradient aligns with the unimodal-transmodal gradient map, suggesting that ongoing brain activity serves as a neuronal baseline via intra- and inter-regional topographic gradients³². Additionally, we ruled out the possibility that the anterior-posterior gradient of sensitivity from semantic to visual features was driven by memory content clustering or qualitative differences (Fig. S7).

Ensuring rigor in subjective report classification. During the procedure, the clinician consistently asked the patient standardized, open-ended questions about the sensations elicited, with follow-up

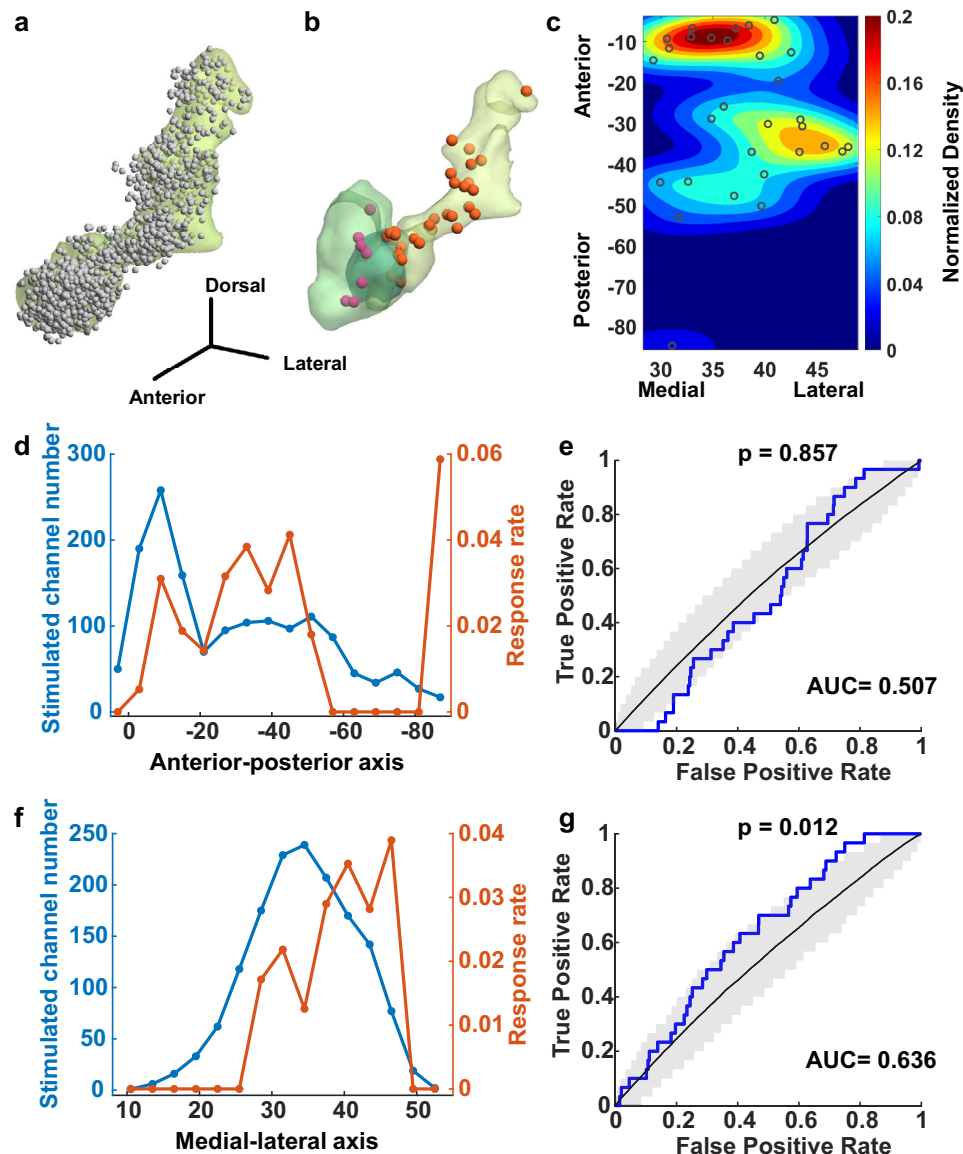


Fig. 4 | Induced reminiscences across the fusiform gyrus. **a** Distribution of 1496 high frequency stimulated sites on the fusiform gyrus from 195 patients. **b** The induced reminiscences in the fusiform gyrus (pale green) and rhinal cortex (sage green), with orange and purple spheres showing sites that induced reminiscences respectively. The dark green portion indicates the overlap of the two regions. **c** Proportion of sites induced reminiscences along anterior-posterior and medial-lateral axes of fusiform gyrus. **d** Stimulated channel number and response rate along the anterior-posterior axis of fusiform gyrus. **e** Receiver operating characteristic (ROC) analysis showing the relationship between responsive/

unresponsive states and distance from the anterior-posterior axis of the fusiform gyrus ($p = 0.857$, $AUC = 0.507$, one-sided permutation test). The black line indicates the mean shuffled ROC curve, and gray shaded areas represent the 95% confidence intervals based on 1000 permutations. **f** Stimulated channel number and response rate along the medial-lateral axis of fusiform gyrus. **g** ROC analysis showing the relationship between responsive/unresponsive states and distance from the medial-lateral axis of the fusiform gyrus ($p = 0.012$, $AUC = 0.636$, one-sided permutation test). Shaded error bands represent 95% confidence intervals. AUC area under the curve. Source data are provided as a Source Data file.

questions as needed to clarify the experience. However, the clinicians may occasionally have asked potentially leading questions during the follow-up inquiry. Notably, any form of leading questions should be strictly avoided in electrical stimulation studies. We meticulously examined all 102 reports pertaining to reminiscences. There were three reports in total that might have been impacted by the clinician (refer to the “Potential Bias Items” worksheet within the raw data file). Although the content of the follow-up questions was not relevant to the current classification, we recruited three additional evaluators to perform the classification. None of them were aware of the purpose of the present research. Based on the statements preceding the potentially leading questions, they independently classified these three subjective reports into different categories. Their classifications were

precisely consistent across all three evaluators, and entirely consistent with the previous evaluations that included the full reports. This further suggests that these three reports did not impact the present findings. Additionally, we analyzed the results after excluding these three reports. The results were entirely consistent with the previous ones, reaffirming the stability of our findings.

Discussion

Based on extensive sampling across the human cortex, we found that internally-oriented reminiscences and externally-oriented hallucinations were primarily elicited after iES of the mesial temporal structures and lateral temporal lobe, including the fusiform gyrus, inferior temporal gyrus, superior temporal pole, hippocampus, and

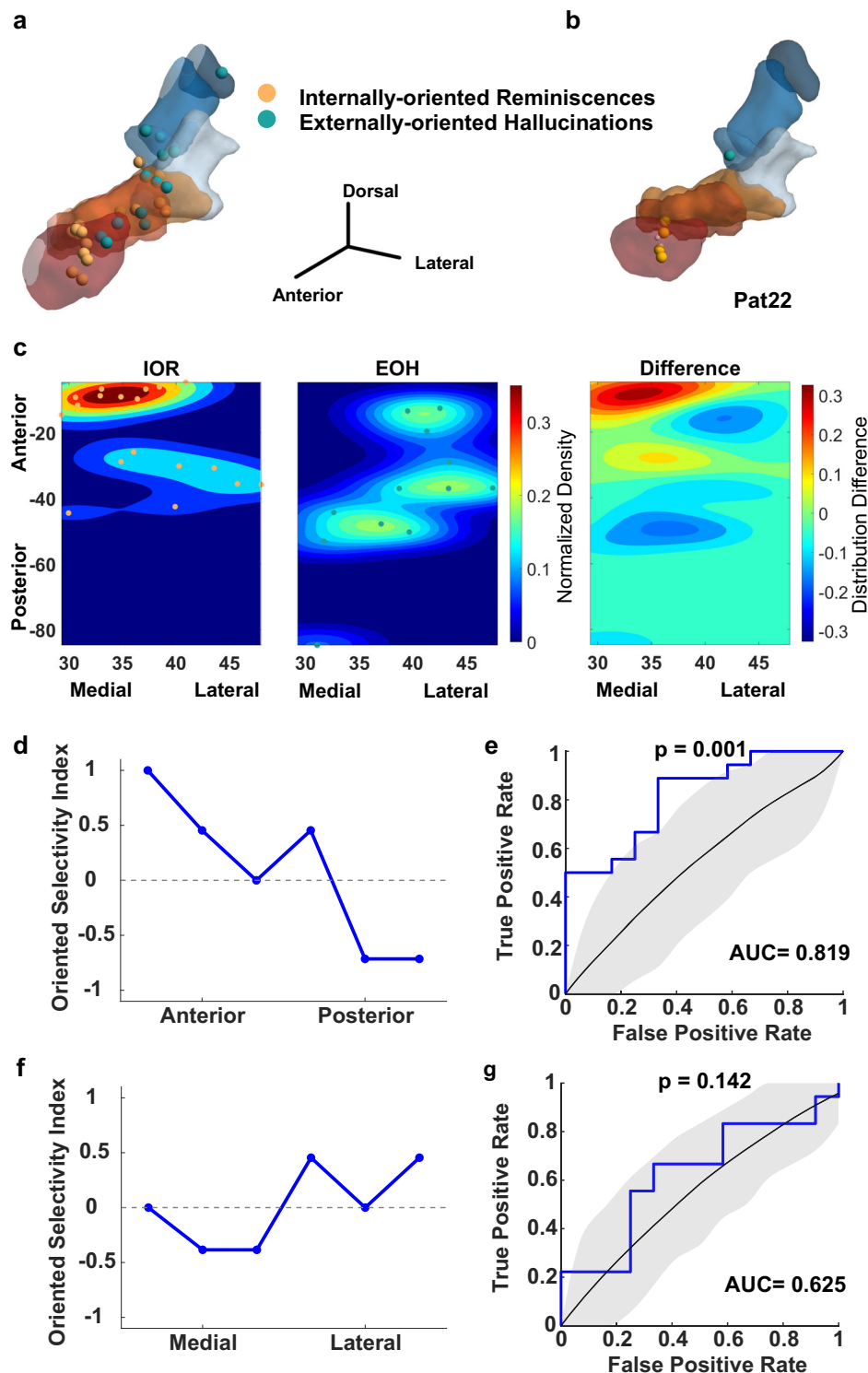


Fig. 5 | The perceptual-mnemonic transition underlying the reconstruction of memories along the fusiform gyrus. **a** Distribution of internally-oriented reminiscences (yellow) and externally-oriented hallucinations (cyan). **b** Distribution of response sites from Patient 22 in the fusiform gyrus. **c** The relative distribution density and differences of memory types along the anterior-posterior and medial-lateral axes of fusiform gyrus. Color-coded values indicate normalized difference in the distribution of internally-oriented reminiscences relative to externally-oriented hallucinations. **d** Oriented selectivity index along the anterior-posterior axis of the fusiform gyrus. Line plot shows the selectivity index, i.e., the differential occurrences between internally-oriented reminiscences and externally-oriented

hallucinations along the anterior-posterior axis of fusiform gyrus. **e** ROC analysis of the relationship between internally-oriented reminiscences/externally-oriented hallucinations and sites from the anterior-posterior axis of the fusiform gyrus ($p = 0.001$, $AUC = 0.819$, one-sided permutation test). **f** Oriented selectivity index along the medial-lateral axis of the fusiform gyrus. **g** ROC analysis of the relationship between internally-oriented reminiscences/externally-oriented hallucinations and sites from the medial-lateral axis of fusiform gyrus ($p = 0.142$, $AUC = 0.625$, one-sided permutation test). Shaded error bands represent 95% confidence intervals. IOR Internally-oriented Reminiscences, EOH Externally-oriented Hallucinations. Source data are provided as a Source Data file.

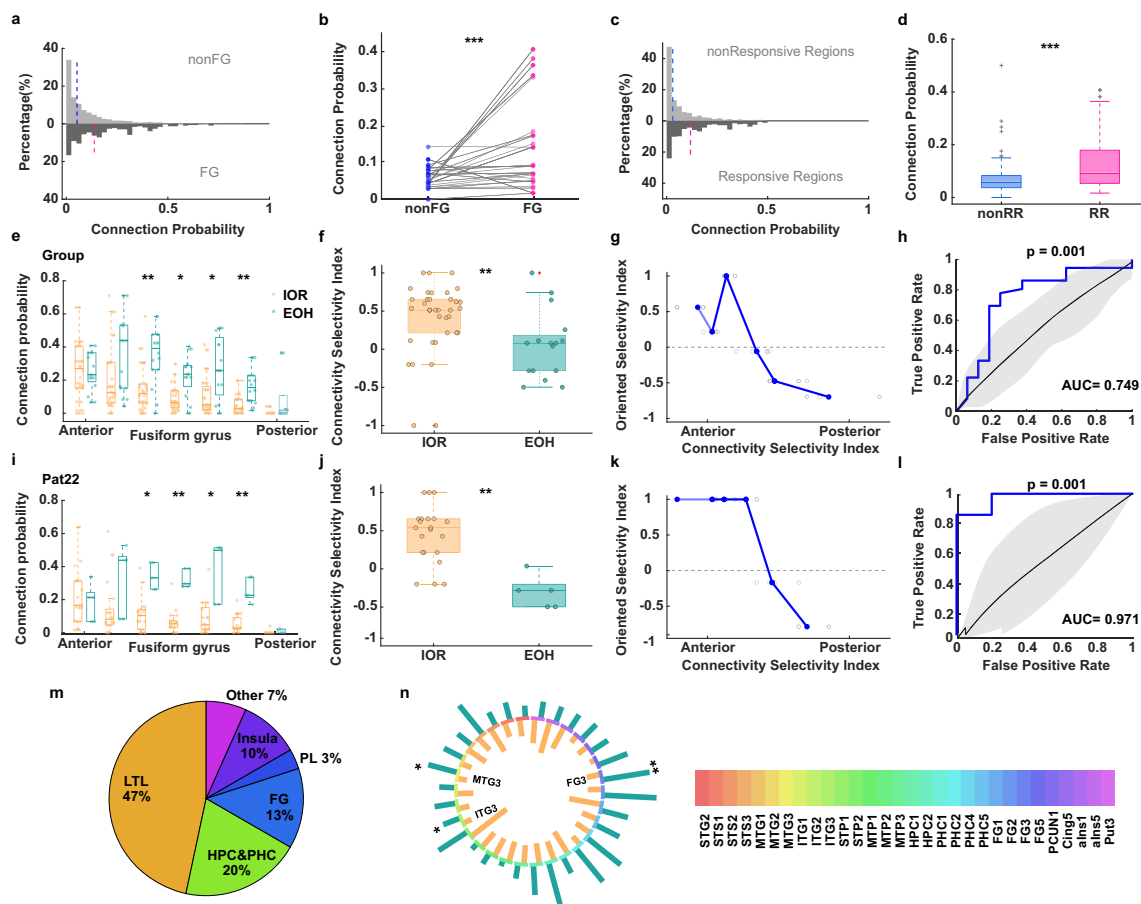


Fig. 6 | Induced reminiscences in non-fusiform regions connected to the fusiform gyrus (FG). **a** Connection probabilities from non-FG sites to both FG and non-FG regions. Pink and blue dashed lines indicate medians. **b** FG connections stronger than non-FG (Two-sided Wilcoxon test: $Z = -4.815$, $p = 1.473 \times 10^{-6}$, $n = 52$). **c**, **d** Responsive regions (RR, $n = 52$) showed stronger FG connectivity than non-responsive regions (nonRR, $n = 143$; $p = 2.086 \times 10^{-11}$, Two-sided Mann-Whitney U test). **e** IOR/EOH sites ($n = 36/16$) differentially connected to FG subregions (Bonferroni-corrected p values anterior to posterior: 1.000, 0.126, 0.002, 0.011, 0.037, 0.002, 0.653; two-sided Mann-Whitney U test). **f** IOR exhibited higher connectivity selectivity than EOH ($p = 0.005$, Two-sided Mann-Whitney U test). **g** Oriented selectivity index along FG's anterior-posterior axis. Gray dots: individual data; blue dots: group medians. **h** ROC analysis of IOR/EOH discrimination via FG anterior-posterior connectivity. Shaded error bands represent 95% confidence intervals. **i** Connection probabilities from IOR and EOH ($n = 21/5$) sites to fusiform subregions in Patient 22 ($n = 26$). Bonferroni-corrected p values (two-sided Mann-Whitney U

test, anterior to posterior: 1.000, 0.717, 0.015, 0.010, 0.042, 0.009, 0.885). **j** Connectivity selectivity index between IOR and EOH in Patient 22 ($p = 0.0014$, two-sided Mann-Whitney U test). **k** The oriented selectivity index along the anterior-posterior axis of FG in Patient 22. **l** ROC analysis distinguishing IOR vs. EOH based on connectivity along the anterior-posterior axis in Patient 22 ($p = 0.001$, AUC = 0.971, one-sided permutation test). **m** Proportion of the top 30 brain regions strongly connected to non-fusiform responsive sites. **n** Distribution of the top 30 probabilities of connections in IOR and EOH, Bonferroni-corrected p values. Numbers in legend indicate subregion positions. IOR Internally-oriented Reminiscences, EOH Externally-oriented Hallucinations, CC Cingulate Cortex, FL Frontal Lobe, LTL Lateral Temporal Lobe, PL Parietal Lobe, Other = regions not classified into these areas. Box plots: center = median; box = 25th–75th percentiles; whiskers = $\pm 1.5 \times$ the interquartile range; outliers plotted individually. Significance: * $p < 0.05$, ** $p < 0.01$, *** $p < 0.001$. Source data are provided as a Source Data file.

parahippocampus. These observations align with prior stimulation studies^{22–27}, intracranial electroencephalogram findings^{3,33} and neuroimaging evidence^{34–36}. More importantly, our findings reveal a causal anterior-posterior functional gradient in the fusiform gyrus, linking perceptual-mnemonic organization to memory reconstruction. Perturbing the neural populations along the anterior-posterior axis of the fusiform gyrus and its upstream regions progressively shifted responses from internally-oriented reminiscences to externally-oriented hallucinations. Our findings provide empirical evidence consistent with the hypothesis of a shared neural coding principle between perception and memory systems³². This theoretical framework suggests that the spatiotemporal dynamics of ongoing neural activity may constitute a common coding mechanism that supports both internally-oriented cognitive processes (e.g., memory retrieval, imagination) and externally-oriented functions (e.g., sensory perception). Notably, this potential shared coding mechanism appears to exhibit a gradient of functional sensitivity along the anterior-posterior

axis, which may reflect the hierarchical organization of the brain's neural information processing along a continuum of internal and external cognition.

Our findings demonstrate that iES-elicited reminiscences are rare mental phenomena characterized by high specificity and predominant localization within the fusiform gyrus, aligning with previous studies that confirm the low prevalence of reminiscence induction through iES, with semantic memories representing the majority of elicited responses²³. The fusiform gyrus, as a higher-order visual processing region, plays a pivotal role in cross-modal information integration³⁷, as evidenced by our investigation of 1496 stimulation sites, which revealed 636 positive responses encompassing various perceptual phenomena (e.g., phosphenes, visual/auditory sensations) and cognitive experiences (e.g., reminiscences, emotions), consistent with the region's transmodal characteristics³⁷. The rarity of iES-induced reminiscences likely reflects fundamental principles of brain network architecture and functional connectivity gradients³⁸. Their rarity may

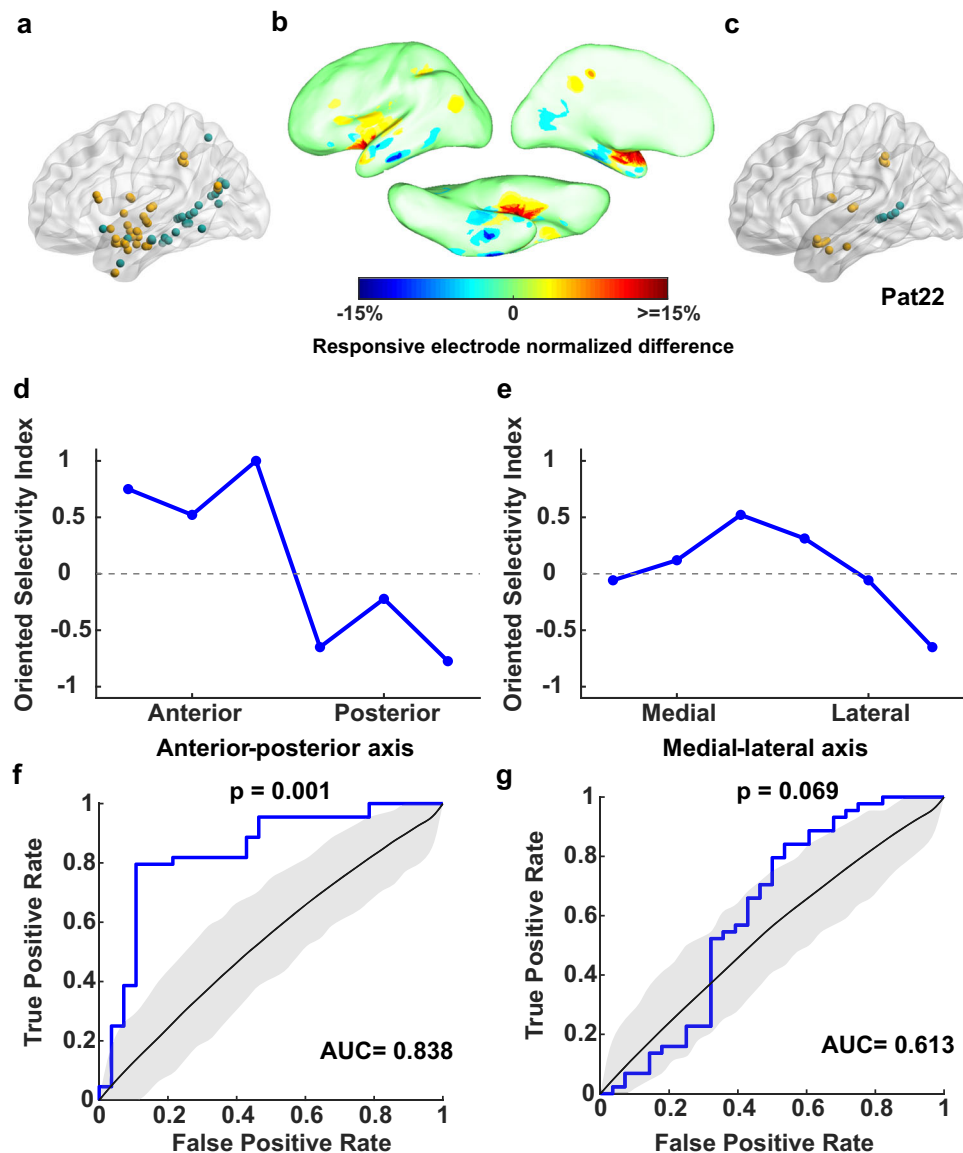


Fig. 7 | The perceptual-mnemonic transition underlying the reconstruction of memories along the anterior-posterior axis in regions outside of the fusiform gyrus. **a** Distribution of responsive sites for internally-oriented reminiscences (yellow) and externally-oriented hallucinations (cyan) outside of the fusiform gyrus. **b** Responsiveness outside the fusiform gyrus rendered on the cortical surface. Color-coded values indicate the normalized differences in responses across the brain surface, with internally-oriented reminiscences shown in warm colors and externally-oriented hallucinations shown in cold colors. **c** Perceptual-mnemonic transition underlying memory reconstruction along the

anterior-posterior axis in regions outside the fusiform gyrus in Patient 22. **d** Oriented selectivity index along the anterior-posterior axis of the brain. **e** Oriented selectivity index along the medial-lateral axis of the brain. **f** ROC analysis of the relationship between internally-oriented reminiscences/externally-oriented hallucinations and sites from the anterior-posterior axis of the brain. **g** ROC analysis of the relationship between internally-oriented reminiscences/externally-oriented hallucinations and sites from the medial-lateral axis of the brain. Shaded error bands represent 95% confidence intervals. Source data are provided as a Source Data file.

be related to current theoretical frameworks suggesting that significant alterations in conscious experience require large-scale perturbation of neuronal populations with high-dimensional, non-specific representations³⁹. However, the localized nature of iES, affecting ~500,000 cells⁴⁰ within brief temporal windows, may be insufficient to meet these requirements, highlighting the complexity of cortical processing attributable to robust inhibitory mechanisms⁴¹, the necessity of coordinated activity across distributed neural networks⁴², and dynamic modulation of theta cycle phase fluctuations during stimulation⁴³. While these findings provide significant insights into the neural correlates of reminiscence, the precise mechanisms underlying iES-induced memory retrieval remain to be fully elucidated, warranting future research to explore the interplay between localized cortical

stimulation, large-scale network dynamics, and the high-dimensional nature of neural representations.

Stimulation of the fusiform gyrus, particularly its middle and anterior sections, induces reminiscences. The fusiform gyrus constitutes a core hub of the cortical network where memories are embedded^{9,13–15,23}. Electrical perturbation of this region triggers involuntary reliving of past experiences as memories are reconstructed²³. Regarding the medial-lateral axis, stimulation of the laterallateral aspect, but not the medial aspect, often induced reminiscences, likely due to cytoarchitectonic differences^{15,16} and receptor density⁴⁴. This is consistent with findings that the mid-fusiform sulcus, which divides the fusiform gyrus into lateral and medial partitions, serves as a functional boundary in numerous functional maps⁴⁵. However, the

number of electrodes in the medial fusiform gyrus was relatively limited in this study, rendering these findings preliminary and requiring replication in future studies.

Remarkably, stimulation of neuronal populations along the anterior-posterior axis of the fusiform gyrus revealed a gradual sensitivity gradient, transitioning from semantic to sensory features of memory. This gradient may reflect specific extrinsic connectivity patterns. The anterior fusiform gyrus is anatomically, functionally, and electrophysiologically connected to the rhinal cortex and hippocampus^{46–48}, regions where previous studies have shown reminiscences predominantly associated with iES^{23,24}. Here, iES of the rhinal cortex mostly induced internally-oriented reminiscences (6/7 electrodes, 85.7%), although the incidence was not significantly higher than in the anterior fusiform gyrus (9/12 electrodes, 75%). Thus, the anterior fusiform gyrus appears to be a key cortical memory node⁹, with neuronal populations critical for semantic memory along an anterior-posterior gradient. In contrast, the middle-posterior fusiform gyrus seems essential for sensory features of memories, consistent with findings showing its involvement in retrieving visual information⁴⁹ and storing previously encountered faces⁵⁰. Finally, the anterior-posterior gradient of sensitivity from semantic to visual features in the fusiform gyrus was independent of memory content or qualitative nature.

In addition, our study reveals novel efferent profiles of mnemonic subregions outside the fusiform gyrus using electrophysiological connectivity maps. Notably, outflow paths from both internally-oriented reminiscences and externally-oriented hallucinations primarily targeted regions such as the lateral temporal lobe, fusiform gyrus, hippocampus, and parahippocampus, which prior studies have implicated in memory recognition⁵¹ and recollection^{3,33,34}. More importantly, internally-oriented reminiscences and externally-oriented hallucinations were shaped by outflow connectivity along the anterior-posterior fusiform gyrus. Specifically, stimulation sites associated with internally-oriented reminiscences exhibited stronger connectivity to the anterior fusiform gyrus, whereas those linked to externally-oriented hallucinations showed greater connectivity to the middle-posterior fusiform gyrus. Thus, our findings suggest that the fusiform gyrus serves as a core hub within the anterior-posterior gradient of perceptual-mnemonic organization, supporting memory reconstruction.

The neural mechanisms underlying long-term memory retrieval, particularly the extent of hippocampal dependency, remain a central topic of debate in neuroscience^{52–54}. According to the long-term consolidation theory, memories initially rely on the hippocampus but gradually become independent of it as neocortical networks take over retrieval^{55,56}. Scene reconstruction theory suggests that although the original memory trace may no longer exist in the hippocampus, the hippocampus remains essential for reconstructing coherent, scene-based remote memories^{52,57}. In contrast, the multiple trace theory (MTT) proposes that recent and remote episodic memories are permanently retained in the hippocampus⁵³. Notably, the observed support for MMT may reflect the inclusion of patients with extensive extra-hippocampal damage, who typically exhibit more profound deficits^{58,59}. In this study, our comprehensive brain-wide investigation provides compelling evidence that electrically induced reminiscences are remarkably sparse and anatomically constrained, with the fusiform gyrus emerging as the principal locus. Although 725 hippocampal sites were stimulated across our dataset, there was no evidence for an increased prevalence of reminiscence arising during hippocampal stimulation relative to other brain regions. Our results best support long-term consolidation theory and fit with reports that patients with hippocampal damage preserve remote episodic remembrance, future imagination, or scene construction^{54,60}.

While our study demonstrates an anterior-posterior gradient of perceptual-mnemonic organization within the fusiform gyrus across a

substantial patient cohort, it is important to acknowledge that the occurrence of iES-induced reminiscences remains relatively rare, as evidenced by both our current findings (0.3% overall, 2.0% in fusiform gyrus) and previous reports²³. This spatial specificity, despite the low overall response rate, underscores the functional specialization of this region in memory processing. Although our study demonstrated an anterior-posterior gradient in the fusiform gyrus related to perceptual-mnemonic organization, we cannot conclusively rule out the potential existence of such boundaries due to methodological limitations, particularly the sparse distribution of elicited reminiscences. Further studies are needed to validate this possibility. It should be noted that the present findings predominantly rely on group-level population data, as elicited reminiscences are rare phenomena with most patients reporting only internally-oriented or externally-oriented hallucinations. There were three patients who reported both internally-oriented reminiscences and externally-oriented hallucinations, two exhibited results consistent with the group-level analysis. Previous studies have demonstrated that abnormal interactions between perception and memory can lead to hallucinations⁶ and recognition impairments^{7,8}. Future studies should characterize how perceptual-mnemonic organization is altered along the anterior-posterior axis of the fusiform gyrus in psychiatric disorders associated with hallucinations and neurological disorders characterized by memory deficits. Although our study utilized 1 Hz stimulation as a control condition, future investigations should implement sham stimulation protocols to more precisely delineate stimulation-induced effects from placebo or expectation-related phenomena. Additionally, it is unclear whether our findings on visual memory reconstruction in the fusiform gyrus generalize to other modalities, such as auditory memory.

In summary, this study found that neural populations along the anterior-posterior axis of the fusiform gyrus, but not the medial-lateral axis, shift in sensitivity from semantic to visual memory features. These findings suggest that the fusiform gyrus may play a key role in integrating perceptual and mnemonic features during memory reconstruction.

Methods

Participants

In this study, we reviewed the responses of reminiscences to 50 Hz electrical stimulation in 335 patients (age range: 4–54 years, mean age \pm standard deviation = 20.8 \pm 9.9 years, 125 females) undergoing intracerebral electroencephalographic (EEG) monitoring for medically refractory epilepsy between January 2016 and June 2023 at the Sanbo Brain Hospital, Capital Medical University, China. According to the inclusion and exclusion criteria (see classifications of reported reminiscences for details), we identified 25 patients (age range: 6–43 years, mean age \pm standard deviation = 22.9 \pm 9.4 years, 7 females) who exhibited memory-related responses upon iES. No significant differences were observed in gender ($\chi^2 = 1.002$, $p = 0.317$, Chi-squared Test) or age ($t = 1.365$, $p = 0.173$, Independent Samples t -test) between the 335 patients and those who exhibited visual memory responses. Clinical information was shown in Supplementary Table 1. Simultaneously, 4971 stimulation contacts from 140 patients (age range: 4–54 years; mean age \pm standard deviation = 20.5 \pm 9.7 years; 56 females) were subjected to 1 Hz stimulation. Among these, 2246 sites were stimulated for a duration of 10 s, while 2725 sites received stimulation for 30 s. None of these stimulations elicited memory-related responses. The specific anatomical subdivisions of the stimulation sites are detailed in Supplementary Table 3. Two neurologists (J.W. and M.Y.W.) confirmed that the stimulated sites eliciting reminiscences were not localized within the epileptogenic zone. Informed consent was obtained from all patients or their guardians, and the study protocol was approved by the Ethical Committee of the Institute of Psychology, Chinese Academy of Sciences (H20034).

Intracranial electrical stimulation procedure

IES was routinely employed to induce partial or complete clinical epileptic seizures and delineate functional areas. We have formulated a rigorous protocol for performing electrical stimulation procedures to ensure the collection of accurate and reliable data. The procedures are summarized as follows:

- 1. Patient positioning and isolation from visual cues:** The patient was seated on the bed facing forward, with their line of sight carefully controlled to prevent any visibility of the operation interface, stimulator, or the clinician's face. This arrangement was intentionally designed to eliminate potential confounding factors, such as inadvertent influence from the clinician's facial expressions or non-verbal cues. The clinician maintained a position that avoided direct visual contact with the patient, ensuring complete isolation from external visual stimuli. This approach was critical to maintaining the objectivity of the patient's responses.
- 2. Blinding of stimulation parameters:** To minimize potential bias in the patient's responses, the specific stimulation parameters, such as current intensity, frequency, and electrode locations, were deliberately concealed from the patient throughout the procedure. This blinding strategy was implemented to ensure that the patient's subjective reports and behavioral responses were solely influenced by the physiological effects of the stimulation, rather than any preconceived expectations or knowledge of the parameters being applied.
- 3. Stimulation administration and documentation:** The clinician systematically adjusted the electrode locations and stimulation parameters in a controlled manner. Each step was rigorously documented, including the precise order of stimulations, the specific parameters applied (e.g., current, frequency, and duration), and any preliminary subjective reports or behavioral changes observed in the patient. This rigorous documentation process was implemented to ensure the accuracy and traceability of the data, thereby facilitating subsequent analysis.
- 4. Standardized patient interaction:** Throughout the procedure, the patient was asked standardized, open-ended questions about their sensations, with follow-up questions used as needed to further clarify and elaborate on the patient's experiences. All interactions, including the clinician's questions and the patient's responses, were recorded via video to ensure accurate documentation.
- 5. Verification and transcription:** A second clinician transcribed the patient's reports and behaviors based on the auditory-visual recordings. Any discrepancies between the preliminary and final reports were immediately addressed by re-examining the video recordings to ensure data accuracy.

The iES was administered using a biphasic electrical stimulator (Nicolet Cortical Stimulator, Middleton, WI). The 50 Hz stimulation consisted of biphasic square-wave pulses (duration = 0.3 or 0.5 ms) applied continuously for 5 s. To control for non-specific effects, some patients received low-frequency stimulation at 1 Hz, which maintained identical pulse characteristics but was delivered for longer durations (10 or 30 s). The same protocols were used for both conditions, differing only in stimulation parameters. Stimulation was immediately terminated upon onset of a clinical response (e.g., pre-seizure aura or epileptic seizure) or EEG after-discharges. Stimulation intensity ranged from 0.1 to 6 mA.

Classifications of reported reminiscences

After electrical stimulation, patients were consistently asked standardized, open-ended questions about the sensations elicited, with follow-up questions as needed to clarify their experiences. All experiential reports related to visual memory elicited by iES were screened. The inclusion criteria for induced visual reminiscences, similar to those

in a previous study²³, were as follows: (1) visual contents that could be more or less elaborate; (2) a clear relation to memory; (3) exclusion of déjà-vu and déjà-vécu phenomena that were devoid of any content or mental imagery; and (4) exclusion of rudimentary visual hallucinations, such as simple phosphenes and shapes unrelated to memory.

Three evaluators (M.T.Y., Y.F.C., and W.Y.Y.) with expertise in psychology and cognitive neuroscience independently categorized the subjective reports into different classifications based on the reported contents. The reminiscences were initially classified by the evaluators independently, and the final category was determined by consensus among the evaluators (Fig. 1b). Reports with inconsistent classifications across evaluators (i.e., those for which consensus could not be reached) were assigned to an “unclassifiable” category. Specifically, reminiscences were categorized along three dimensions: source, content, and quality. The source dimension differentiated whether the induced experiential phenomena originated from internally-oriented reminiscences or externally-oriented hallucinations. The internally-oriented reminiscences denoted reactions perceived by patients as remembering past experiences or familiar people in their mind, while externally-oriented one signified experiences perceived as occurring in the field of vision. Content categorization divided reminiscences into six subtypes: scenes, people, animals, objects, scenes with people, and unclassifiable. Additionally, we classified reminiscences based on modern conceptions of memory³¹, following the classification criteria outlined by Curot et al.²³, resulting in four final categories: semantic memories, personal semantics, familiarity, and unclassified. Inter-rater agreement was notably high, with initial independent evaluations achieving agreement rates of 92.2%, 85.3%, and 82.4% for the source, content, and quality classifications, respectively. For instance: Patient: I see someone over there soaking a biscuit and eating it. Clinician: Did you feel it in your mind, or did you actually see it in front of you? Patient: In my mind. Clinician: A person appeared in your mind soaking a biscuit and eating it? Patient: Yeah, that's right. Clinician: Is it someone you know? Patient: It seems like someone I know. Clinician: Can you say the person's name? Patient: No. Clinician: It seems like someone you know? Patient: Yes. This report was categorized as “internally-oriented reminiscences”, “scenes & people” and “familiarity”.

Electrode implantation and localization

The selection of intracranial electrode locations was determined with the objective of identifying the epileptogenic zone and functionally eloquent areas. This decision was made collaboratively by a multi-disciplinary team comprising neurologists and neurosurgeons. Electrode coordinates were obtained using a semi-automated approach⁶¹. Briefly, electrode contacts (0.8 mm in diameter, 2 mm in long, and 1.5 mm apart; Beijing Huakehengsheng Healthcare Corporation Ltd., Beijing, China) were localized based on the patient's preoperative MR imaging (MRI) co-registered with their postoperative computed tomography (CT) image. The electrode clusters within co-registered CT were then automatically detected and visually verified. The coordinates of electrode contacts were calculated based on the trajectory of detected electrode clusters in the native space. Finally, the coordinates of stimulated sites were transformed into the MNI standard space based on the combined volumetric- and surface-based normalization between native structural images and the MNI standard brain⁶². All electrodes were subsequently grouped into regions according to the parcellation scheme of the Atlas of Intrinsic Connectivity of Homotopic Areas (AICHA)⁶³ and Brodmann areas⁶⁴.

Cortical responsiveness and regions of interest parcellation

Memory responses to electrical stimulation were depicted on the cortical surface in a vertex-wise manner. For each cortical vertex, responsiveness was defined as either the number or percentage of memory responsive sites within a 10 mm-radius sphere surrounding

the vertex. We also conducted region of interest (ROI) analyses using the AICHA⁶³ to delineate the topography of different classifications of reminiscences. Previous reports have shown that the rhinal cortex (entorhinal and perirhinal cortices), just anterior to the fusiform gyrus, played a crucial role in perceptual-mnemonic organization⁶⁵ and reminiscences^{23,24}. Here we delineated the rhinal cortex as Brodmann areas 28, 34, 35, and 36⁶⁴. A site was assigned to an ROI if the minimum distance from that site to any voxel within the ROI was less than 4 mm accounting for the local diffusion effect of bipolar electrical stimulation.

Multivariate analysis using linear mixed effects models

The multivariate analysis was performed using a linear mixed effects (LME) model with random intercepts and fixed slopes to identify critical regions associated with reminiscence, while controlling for potential confounding variables. The full models incorporated patient ID as a random effect to account for between-patient variability, with region, age, gender, and stimulation intensity included as fixed effects. The LME model can be expressed as: $\text{Positive Response}_{ij} = \beta_0 + \beta_1 \cdot \text{Region}_j + \beta_2 \cdot \text{Age}_i + \beta_3 \cdot \text{Gender}_i + \beta_4 \cdot \text{CurrentIntensity}_i + u_i + \epsilon_{ij}$

where $\text{Positive Response}_{ij}$ represents the response of individual i in region j , β_0 is the intercept, β_1 through β_4 are the fixed effects for region, age, gender, and stimulation intensity, respectively, u_i is the random effect for patient i , and ϵ_{ij} is the residual error. This analytical approach follows the framework proposed by Yu et al.⁶⁶, where fixed effects estimate population-level parameters, while random effects capture patient-specific variations. Consequently, our findings regarding regional specialization represent robust population-level effects rather than individual idiosyncrasies. Specifically, we integrated AICHA subdivisions (e.g., merging hippocampus 1 and 2 into a unified hippocampus) and calculated LME models for these combined regions (with a significance threshold of $p < 0.05$). The results of the LME models were further corrected for multiple comparisons using the Bonferroni method. To facilitate inter-region comparisons, the region with the lowest response rate was designated as the reference region.

Quantitative analysis of memory responsiveness along spatial axes

To investigate the spatial organization of memory responsiveness along the anterior-posterior axis (Y-axis in the standardized coordinate system) of the fusiform gyrus, we projected reminiscence sites based on their Y-axis coordinates. These coordinates were sorted and divided into six equally sized groups. Within each group, we calculated the response selectivity index between internally-oriented reminiscences and externally-oriented hallucinations using the following formula:

$$\text{Oriented Selectivity Index} = \frac{(N_{\text{internally oriented}} - N_{\text{externally oriented}})}{(N_{\text{internally oriented}} + N_{\text{externally oriented}})}$$

where N represents the proportion of a specific type of reminiscence.

As a control, we replicated this analysis along the medial-lateral axis of the fusiform gyrus to ensure that the observed effects were specific to the anterior-posterior axis. To verify that the results were not dependent on the size of the subgroups, we repeated the analysis by dividing the reminiscence sites into 3, 5, and 10 groups, respectively. This approach allowed us to assess the robustness of our findings across different spatial resolutions.

To systematically examine the potential association between anatomical positions along the anterior-posterior axis of the fusiform gyrus and memory classification performance, we implemented a comprehensive analytical approach using ROC analysis. Specifically, we calculated the area under the curve (AUC) using a generalized linear model (GLM) with binomial distribution to quantify the model's predictive accuracy. To establish statistical significance, we conducted a rigorous permutation test ($n=1000$ iterations), in which we

randomly shuffled the position labels (X-axis: medial-lateral dimension; Y-axis: anterior-posterior dimension) to generate a robust null distribution of AUC values. To account for potential confounding factors, we incorporated covariates into the analysis. Memory content, quality, and individual factors such as gender, age, and stimulation current intensity were included as covariates to control for variability in memory responses that might be attributable to these variables. After integrating these covariates, the AUC was recalculated using the modified GLM, and the permutation procedure was repeated. The statistical significance of our observed AUC was determined by comparing it against this null distribution, with the p value calculated as the proportion of permuted AUC values that were equal to or exceeded the observed AUC (Fig. S8).

Additionally, we applied the same method to examine the perceptual-mnemonic transition underlying memory reconstruction along the anterior-posterior axis in regions outside the fusiform gyrus. This extended analysis provided further insights into the spatial organization of memory-related processes across different brain regions.

Spatial clustering analysis using Euclidean distance

To quantify the spatial organization of memory sites, we employed Euclidean distance as a measure of the straight-line distance between two points in three-dimensional space. Euclidean distance is used to measure the straight-line distance between two points in space. The formula is: $d = \sqrt{(x_a - x_b)^2 + (y_a - y_b)^2 + (z_a - z_b)^2}$. For each content category, the brain coordinates of all memory sites within that category were extracted. For each pair of sites within the category, the Euclidean distance was calculated. For memory sites between different content categories, the Euclidean distance for each pair of sites between categories was also calculated. Specifically, for each pair of categories (e.g., scene and object), the Euclidean distance was computed for all paired sites between the categories. The median of these distances was used to quantify spatial clustering within each category.

To compare the spatial organization of internally-oriented reminiscences and externally-oriented hallucinations, we assessed the differences in Euclidean distances using the Mann-Whitney U test. A significance threshold of $p < 0.05$ was used to determine statistical significance.

Causal connectivity probability from the functional tractography project (F-TRACT)

The probabilistic connectivity of stimulated sites to other regions were achieved using the public dataset of 625 implantations in 613 patients from the F-TRACT (<https://f-tract.eu>, F-TRACT_P_01_v2307). Single pulse electrical stimulation was used to induce cortico-cortical evoked potentials (CCEP), which can be used to infer a large-scale causal connectivity^{29,30}. The connectivity probability was calculated by averaging binary responses across multiple electrode contacts and patients. A binary response of 1 was assigned when a significant CCEP was detected within the first 200 ms after stimulation, and 0 otherwise. The significant response was determined by comparing the Z-scored CCEP amplitude to a threshold, typically a Z-score of five. To transfer the data to a group level, the binary responses and features of CCEPs were averaged at the brain region level, where features like onset latency, peak latency, and amplitude were aggregated by computing the median for each parcel. Connectivity probabilities between each pair of stimulated and recorded parcels were then calculated as the average of binary responses across all relevant contacts. This probability represents the likelihood of observing a significant CCEP response in a given parcel when another parcel is stimulated. The probability values used in this analysis quantify the likelihood of a significant response based on a predefined statistical threshold. Based on the F-TRACT AICHA parcellation-based atlas of probability, we

derived probabilities of connections from responsive sites to other regions. Subsequent aggregation of connectivity probabilities at the individual electrode level yielded the results at the group level.

Since F-TRACT is a probabilistic connectivity map derived from adult patient data, our causal connectivity calculations were restricted to the sites from 11 adult patients, specifically 52 responsive sites. We extracted the row information of the corresponding connectivity probability matrix for each stimulation site based on its brain region, where the corresponding column information represents the connection probability from the stimulation site to other regions. NaN values represent missing or undefined data entries in the matrix. These result from either insufficient stimulation-recording pairs ($N \leq 10$ or significant recordings ≤ 10) or the absence of a white matter connection between two parcels. To ensure reliability when ranking connection probabilities, we filtered brain regions to include only those with valid connectivity values from at least 70% of stimulation sites. To ensure that the results were not sensitive to this threshold, we repeated our analysis using 60% and 80% valid connectivity thresholds. These regions were ranked according to the median of their probabilities, and the top 30 regions were selected to identify connectivity differences associated with different types of reminiscences from regions with inherently stronger connection probabilities (Fig. S9).

Statistical methods for distribution comparison

The Kolmogorov-Smirnov (KS) test was used to compare the distributions of response area probabilities connected to the fusiform gyrus (FG) with those of non-fusiform areas (nonFG), as well as the distributions of non-responsive regions (nonRR) connected to the fusiform gyrus. The KS test is a non-parametric method that evaluates whether two samples are drawn from the same distribution by measuring the maximum absolute difference between their cumulative distribution functions (referred to as the D value). In this study, the KS test was applied to assess distributional differences between experimental conditions, with a significance threshold set at $p < 0.05$.

The median was chosen for its robustness against outliers and its effectiveness in representing the central tendency of the data. To compare the median probability of connections between the fusiform gyrus and non-fusiform regions, we used the Wilcoxon signed-rank test. This test was selected because it is appropriate for paired data and does not require the assumption of normality. Prior to analysis, the data distribution was assessed using histograms, which confirmed a non-normal distribution. We also verified that all test assumptions were met, including: the requirement for paired observations, the absence of significant outliers. The null hypothesis (H_0) stated that there would be no significant difference in the median connection probabilities between the fusiform gyrus and non-fusiform regions, while the alternative hypothesis (H_1) posited that a significant difference would exist. A significance threshold of $p < 0.05$ was applied.

For comparisons between regions with and without responses projecting to the fusiform gyrus, the Mann-Whitney U test was employed. This test is suitable for independent samples and does not require normally distributed data. Before conducting the test, we confirmed that the assumptions of independent observations and ordinal or continuous data were met. The null hypothesis (H_0) assumed no significant difference in the median connection probabilities between regions with and without responses projecting to the fusiform gyrus, while the alternative hypothesis (H_1) suggested that a significant difference would exist. A significance threshold of $p < 0.05$ was used.

Connectivity selectivity analysis along the anterior-posterior axis of the fusiform gyrus

To investigate whether the efferents from other stimulated sites to the fusiform gyrus exhibited distinct connectivity patterns associated with internally-oriented reminiscences and externally-

oriented hallucinations, we calculated the connectivity selectivity index. This index quantifies the preferential connectivity of stimulated sites to the anterior versus middle-posterior regions of the fusiform gyrus. The connectivity selectivity index was calculated based on this equation: $(P_{\text{FGA}} - P_{\text{FGP}}) / (P_{\text{FGA}} + P_{\text{FGP}})$. Here, P_{FGA} represents the connection probability to the anterior fusiform gyrus (i.e., fusiform gyrus 1 in the AICHA atlas), while P_{FGP} represents the median connection probability to the middle-posterior fusiform gyrus (i.e., fusiform gyrus 2-7).

The Mann-Whitney U test was applied to compare the connection probabilities from regions associated with internally-oriented reminiscences and externally-oriented hallucinations to each subregion of the fusiform gyrus. To account for multiple comparisons across FG subregions ($n = 7$), a Bonferroni correction was applied, with the significance threshold set at $p < 0.05$. Additionally, the Mann-Whitney U test was used to assess differences in the connection selectivity index between internally-oriented reminiscences and externally-oriented hallucinations.

To evaluate the influence of upstream cortical structures on memory classifications along the anterior-posterior fusiform gyrus, the connectivity selectivity index labels were shuffled in order to generate a null distribution for comparison. The observed AUC was then compared to this null distribution to assess statistical significance, with p values calculated as described above. To control for potential confounding factors, covariates including memory content, quality, and individual factors such as gender, age, and stimulation current intensity were incorporated into the analysis. After integrating these covariates, the AUC was recalculated using the modified GLM, and the permutation procedure was repeated to ensure robustness. The statistical significance of the updated model was reassessed using the permutation test, with p values derived from the distribution of AUC values obtained through label shuffling.

Reporting summary

Further information on research design is available in the Nature Portfolio Reporting Summary linked to this article.

Data availability

The raw data, including complete reports of induced reminiscences with stimulation intensities and their classifications (source, content, and quality), and the anatomical locations of all responsive sites (MNI coordinates with AICHA labels), are available at <https://doi.org/10.5281/zenodo.15813710>. The processed data in this study can be accessed via: <https://doi.org/10.5281/zenodo.15797927>. Source data are provided with this paper.

Code availability

The code used for this study is available at <https://github.com/randomquestve/code.git>, and has been archived with the <https://doi.org/10.5281/zenodo.15801774>.

References

1. Kiyonaga, A., Scimeca, J. M., Bliss, D. P. & Whitney, D. Serial dependence across perception, attention, and memory. *Trends Cogn. Sci.* **21**, 493–497 (2017).
2. Libby, A. & Buschman, T. J. Rotational dynamics reduce interference between sensory and memory representations. *Nat. Neurosci.* **24**, 715–726 (2021).
3. Mohan, U. R., Zhang, H., Ermentrout, B. & Jacobs J. The direction of theta and alpha travelling waves modulates human memory processing. *Nat. Hum. Behav.* **8**, 1124–1135 (2024).
4. Rademaker, R. L., Chunharas, C. & Serences, J. T. Coexisting representations of sensory and mnemonic information in human visual cortex. *Nat. Neurosci.* **22**, 1336–1344 (2019).

5. Steel, A., Silson, E. H., Garcia, B. D. & Robertson, C. E. A retinotopic code structures the interaction between perception and memory systems. *Nat. Neurosci.* **27**, 339–347 (2024).
6. Diederer, K. M. et al. Deactivation of the parahippocampal gyrus preceding auditory hallucinations in schizophrenia. *Am. J. Psychiatry* **167**, 427–435 (2010).
7. Stothart, G., Smith, L. J., Milton, A. & Coulthard, E. A passive and objective measure of recognition memory in Alzheimer's disease using Fastball memory assessment. *Brain* **144**, 2812–2825 (2021).
8. Tennant, V. R. et al. Fusiform gyrus phospho-tau is associated with failure of proper name retrieval in aging. *Ann. Neurol.* **90**, 988–993 (2021).
9. Rossion, B., Jacques, C. & Jonas, J. The anterior fusiform gyrus: the ghost in the cortical face machine. *Neurosci. Biobehav. Rev.* **158**, 105535 (2024).
10. Silson, E. H. et al. A posterior-anterior distinction between scene perception and scene construction in human medial parietal cortex. *J. Neurosci.* **39**, 705–717 (2019).
11. Haxby, J. V. et al. Distributed and overlapping representations of faces and objects in ventral temporal cortex. *Science* **293**, 2425–2430 (2001).
12. Haxby, J. V. et al. A common, high-dimensional model of the representational space in human ventral temporal cortex. *Neuron* **72**, 404–416 (2011).
13. Mion, M. et al. What the left and right anterior fusiform gyri tell us about semantic memory. *Brain* **133**, 3256–3268 (2010).
14. Hodges, J. R. & Patterson, K. Semantic dementia: a unique clinicopathological syndrome. *Lancet Neurol.* **6**, 1004–1014 (2007).
15. Weiner, K. S. & Zilles, K. The anatomical and functional specialization of the fusiform gyrus. *Neuropsychologia* **83**, 48–62 (2016).
16. Weiner, K. S. The Mid-Fusiform Sulcus (sulcus sagittalis gyri fusiformis). *Anat. Rec.* **302**, 1491–1503 (2019).
17. Parvizi, J. et al. Electrical stimulation of human fusiform face-selective regions distorts face perception. *J. Neurosci.* **32**, 14915–14920 (2012).
18. Rangarajan, V. et al. Electrical stimulation of the left and right human fusiform gyrus causes different effects in conscious face perception. *J. Neurosci.* **34**, 12828–12836 (2014).
19. Jonas, J. et al. A face identity hallucination (palinopsia) generated by intracerebral stimulation of the face-selective right lateral fusiform cortex. *Cortex* **99**, 296–310 (2018).
20. Jonas, J. et al. Beyond the core face-processing network: Intracerebral stimulation of a face-selective area in the right anterior fusiform gyrus elicits transient prosopagnosia. *Cortex* **72**, 140–155 (2015).
21. Volfart, A. et al. Intracerebral electrical stimulation of the right anterior fusiform gyrus impairs human face identity recognition. *Neuroimage* **250**, 118932 (2022).
22. Penfield, W. Some mechanisms of consciousness discovered during electrical stimulation of the brain. *Proc. Natl. Acad. Sci. USA* **44**, 51–66 (1958).
23. Curot, J. et al. Memory scrutinized through electrical brain stimulation: a review of 80 years of experiential phenomena. *Neurosci. Biobehav. Rev.* **78**, 161–177 (2017).
24. Gillinder, L., Liegeois-Chauvel, C. & Chauvel, P. What déjà vu and the “dreamy state” tell us about episodic memory networks. *Clin. Neurophysiol.* **136**, 173–181 (2022).
25. Gloor, P. Experiential phenomena of temporal lobe epilepsy. Facts and hypotheses. *Brain* **113**, 1673–1694 (1990).
26. Bartolomei, F. et al. Cortical stimulation study of the role of rhinal cortex in déjà vu and reminiscence of memories. *Neurology* **63**, 858–864 (2004).
27. Halgren, E., Walter, R. D., Cherlow, D. G. & Crandall, P. H. Mental phenomena evoked by electrical stimulation of the human hippocampal formation and amygdala. *Brain* **101**, 83–117 (1978).
28. Sjöberg, R. L. Brain stimulation and elicited memories. *Acta Neurochir.* **165**, 2737–2745 (2023).
29. David, O. et al. Probabilistic functional tractography of the human cortex. *Neuroimage* **80**, 307–317 (2013).
30. Trebault, L. et al. Probabilistic functional tractography of the human cortex revisited. *Neuroimage* **181**, 414–429 (2018).
31. Renoult, L., Davidson, P. S., Palombo, D. J., Moscovitch, M. & Levine, B. Personal semantics: at the crossroads of semantic and episodic memory. *Trends Cogn. Sci.* **16**, 550–558 (2012).
32. Northoff, G., Vatansever, D., Scalabrini, A. & Stamatakis, E. A. Ongoing brain activity and its role in cognition: dual versus baseline models. *Neuroscientist* **29**, 393–420 (2023).
33. Norman, Y., Raccach, O., Liu, S., Parvizi, J. & Malach, R. Hippocampal ripples and their coordinated dialogue with the default mode network during recent and remote recollection. *Neuron* **109**, 2767–2780.e2765 (2021).
34. Polyn, S. M., Natu, V. S., Cohen, J. D. & Norman, K. A. Category-specific cortical activity precedes retrieval during memory search. *Science* **310**, 1963–1966 (2005).
35. Ranganath, C. & Ritchey, M. Two cortical systems for memory-guided behaviour. *Nat. Rev. Neurosci.* **13**, 713–726 (2012).
36. Simons, J. S., Ritchey, M. & Fernyhough, C. Brain mechanisms underlying the subjective experience of remembering. *Annu. Rev. Psychol.* **73**, 159–186 (2022).
37. von Kriegstein, K., Kleinschmidt, A., Sterzer, P. & Giraud, A. L. Interaction of face and voice areas during speaker recognition. *J. Cogn. Neurosci.* **17**, 367–376 (2005).
38. Fox, K. C. R. et al. Intrinsic network architecture predicts the effects elicited by intracranial electrical stimulation of the human brain. *Nat. Hum. Behav.* **4**, 1039–1052 (2020).
39. Odegaard, B., Knight, R. T. & Lau, H. Should a few null findings falsify prefrontal theories of conscious perception? *J. Neurosci.* **37**, 9593–9602 (2017).
40. Parvizi, J. & Kastner, S. Promises and limitations of human intracranial electroencephalography. *Nat. Neurosci.* **21**, 474–483 (2018).
41. Isaacson, J. S. & Scanziani, M. How inhibition shapes cortical activity. *Neuron* **72**, 231–243 (2011).
42. Harris, K. D. & Mrsic-Flogel, T. D. Cortical connectivity and sensory coding. *Nature* **503**, 51–58 (2013).
43. Rutishauser, U., Ross, I. B., Mamelak, A. N. & Schuman, E. M. Human memory strength is predicted by theta-frequency phase-locking of single neurons. *Nature* **464**, 903–907 (2010).
44. Caspers, J. et al. Receptor architecture of visual areas in the face and word-form recognition region of the posterior fusiform gyrus. *Brain Struct. Funct.* **220**, 205–219 (2015).
45. Grill-Spector, K. & Weiner, K. S. The functional architecture of the ventral temporal cortex and its role in categorization. *Nat. Rev. Neurosci.* **15**, 536–548 (2014).
46. Catenoix, H., Magnin, M., Mauguier, F. & Ryvlin, P. Evoked potential study of hippocampal efferent projections in the human brain. *Clin. Neurophysiol.* **122**, 2488–2497 (2011).
47. Zhang, W. et al. Functional organization of the fusiform gyrus revealed with connectivity profiles. *Hum. Brain Mapp.* **37**, 3003–3016 (2016).
48. Libby, L. A., Ekstrom, A. D., Ragland, J. D. & Ranganath, C. Differential connectivity of perirhinal and parahippocampal cortices within human hippocampal subregions revealed by high-resolution functional imaging. *J. Neurosci.* **32**, 6550–6560 (2012).
49. Wheeler, M. E., Petersen, S. E. & Buckner, R. L. Memory's echo: vivid remembering reactivates sensory-specific cortex. *Proc. Natl. Acad. Sci. USA* **97**, 11125–11129 (2000).
50. Rossion, B. et al. A network of occipito-temporal face-sensitive areas besides the right middle fusiform gyrus is necessary for normal face processing. *Brain* **126**, 2381–2395 (2003).

51. Norman, K. A. & O'Reilly, R. C. Modeling hippocampal and neocortical contributions to recognition memory: a complementary-learning-systems approach. *Psychol. Rev.* **110**, 611–646 (2003).
52. Barry, D. N. & Maguire, E. A. Remote memory and the hippocampus: a constructive critique. *Trends Cogn. Sci.* **23**, 128–142 (2019).
53. Nadel, L., Samsonovich, A., Ryan, L. & Moscovitch, M. Multiple trace theory of human memory: computational, neuroimaging, and neuropsychological results. *Hippocampus* **10**, 352–368 (2000).
54. Dede, A. J., Wixted, J. T., Hopkins, R. O. & Squire, L. R. Autobiographical memory, future imagining, and the medial temporal lobe. *Proc. Natl. Acad. Sci. USA* **113**, 13474–13479 (2016).
55. Squire, L. R., Genzel, L., Wixted, J. T. & Morris, R. G. Memory consolidation. *Cold Spring Harb. Perspect. Biol.* **7**, a021766 (2015).
56. Dede, A. J. O. & Smith, C. N. The functional and structural neuroanatomy of systems consolidation for autobiographical and semantic memory. *Curr. Top. Behav. Neurosci.* **37**, 119–150 (2018).
57. Maguire, E. A. & Mullally, S. L. The hippocampus: a manifesto for change. *J. Exp. Psychol. Gen.* **142**, 1180–1189 (2013).
58. Rosenbaum, R. S. et al. Patterns of autobiographical memory loss in medial-temporal lobe amnesic patients. *J. Cogn. Neurosci.* **20**, 1490–1506 (2008).
59. Gao, A. F. et al. Neuropathology of a remarkable case of memory impairment informs human memory. *Neuropsychologia* **140**, 107342 (2020).
60. Kim, S., Dede, A. J., Hopkins, R. O. & Squire, L. R. Memory, scene construction, and the human hippocampus. *Proc. Natl. Acad. Sci. USA* **112**, 4767–4772 (2015).
61. Qin, C. et al. Automatic and precise localization and cortical labeling of subdural and depth intracranial electrodes. *Front. Neuroinform* **11**, 10 (2017).
62. Postelnicu, G., Zollei, L. & Fischl, B. Combined volumetric and surface registration. *IEEE Trans. Med. Imaging* **28**, 508–522 (2009).
63. Joliot, M. et al. AICHA: an atlas of intrinsic connectivity of homotopic areas. *J. Neurosci. Methods* **254**, 46–59 (2015).
64. Brodmann, K. *Vergleichende Lokalisationslehre der Grosshirnrinde in ihren Prinzipien dargestellt auf Grund des Zellenbaues* (J. A. Barth, 1909).
65. Bussey, T. J. & Saksida, L. M. Object memory and perception in the medial temporal lobe: an alternative approach. *Curr. Opin. Neurobiol.* **15**, 730–737 (2005).
66. Yu, Z. et al. Beyond t test and ANOVA: applications of mixed-effects models for more rigorous statistical analysis in neuroscience research. *Neuron* **110**, 21–35 (2022).

Acknowledgements

We are grateful to all the patients who participated in this study. We are thankful to Huanhuan Xiang, Nan Guan and Pan Kang for their help in collecting the data. This study was supported by the National Natural Science Foundation of China (32020103009, 32471110), STI2030-Major Projects (2022ZD0205000), the Ministry Key Project (GW089000), the

Scientific Foundation of the Institute of Psychology, Chinese Academy of Sciences (E2CX4215CX), CAAE Epilepsy Research Fund-UCB Fund (CU-2023-052).

Author contributions

Y.Y.L. and L.W. conceived, designed, and interpreted the study. J.W. and M.Y.W. collected the data. M.T.Y., Y.F.C., and W.Y.Y. categorized the subjective reports. M.T.Y., Y.Y.L., and B.Z. analyzed the data. Y.Y.L., M.T.Y., L.W., G.N., G.M.L. and H.W.S. wrote the manuscript.

Competing interests

The authors declare no competing interests.

Additional information

Supplementary information The online version contains supplementary material available at

<https://doi.org/10.1038/s41467-025-62561-9>.

Correspondence and requests for materials should be addressed to Liang Wang.

Peer review information *Nature Communications* thanks the anonymous reviewer(s) for their contribution to the peer review of this work. A peer review file is available.

Reprints and permissions information is available at <http://www.nature.com/reprints>

Publisher's note Springer Nature remains neutral with regard to jurisdictional claims in published maps and institutional affiliations.

Open Access This article is licensed under a Creative Commons Attribution-NonCommercial-NoDerivatives 4.0 International License, which permits any non-commercial use, sharing, distribution and reproduction in any medium or format, as long as you give appropriate credit to the original author(s) and the source, provide a link to the Creative Commons licence, and indicate if you modified the licensed material. You do not have permission under this licence to share adapted material derived from this article or parts of it. The images or other third party material in this article are included in the article's Creative Commons licence, unless indicated otherwise in a credit line to the material. If material is not included in the article's Creative Commons licence and your intended use is not permitted by statutory regulation or exceeds the permitted use, you will need to obtain permission directly from the copyright holder. To view a copy of this licence, visit <http://creativecommons.org/licenses/by-nc-nd/4.0/>.

© The Author(s) 2025

¹State Key Laboratory of Cognitive Science and Mental Health, Institute of Psychology, Chinese Academy of Sciences, Beijing, China. ²School of Psychology, Shandong Second Medical University, Shandong, China. ³Department of Psychology, University of Chinese Academy of Sciences, Beijing, China. ⁴Department of Neurology, SanBo Brain Hospital, Capital Medical University, Beijing, China. ⁵School of Education, Beijing Institute of Technology, Beijing, China. ⁶Key Laboratory of Brain Science, Zunyi Medical University, Zunyi, China. ⁷Guizhou Key Laboratory of Anesthesia and Organ Protection, Zunyi Medical University, Zunyi, China. ⁸Department of Neurosurgery, SanBo Brain Hospital, Capital Medical University, Beijing, China. ⁹Mind, Brain Imaging and Neuroethics Research Unit, The Royal's Institute of Mental Health Research associated with The University of Ottawa, Ottawa, ON, Canada. ¹⁰These authors contributed equally: Motong Yuan, Yanyan Li. ✉ e-mail: lwang@psych.ac.cn